2008-5435/14/63-1-8
INTERNATIONAL JOURNAL OF OCCUPATIONAL HYGIENE

IJOH 10: 124-134, 2018

ORIGINAL ARTICLE

Fumed Silica Particle Deagglomeration Associated with Instrument Techniques

JARED KHATTAK[1], NARA SHIN[1], WENDELL E. RHINE[2], GEORGE L. GOULD[2], CANDACE S.J. TSAI[1*]

[1]*Department of Environmental and Radiological Health Sciences, College of Veterinary Medicine and Biomedical Sciences, Colorado State University, 1681 Campus Delivery, Fort Collins, CO 80523*
[2]*Aspen Aerogels, Inc., 30 Forbes Road, Northborough, MA 01532*

Received April 14, 2017; Revised July 26, 2018; Accepted August 20, 2018

This paper is available on-line at *http://ijoh.tums.ac.ir*

ABSTRACT

Fumed silica, due to the thixotropic properties and low thermal conductivity, is used in insulation products. Exposure to crystalline silica is of most concern and there is also evidence that exposure to nanometer-sized fumed silica may lead to adverse health outcomes. Workers' exposure to aerosolized fumed silica and other potentially hazardous materials are commonly assessed using direct-reading instruments. These instruments often contain an aerosol pre-separator cyclone, which by dispersing agglomerated particles, may cause variations in the reading values. This study investigates the effect of these cyclones on the measurements by comparing three instruments for airborne fumed silica that was generated using manual and automatic manipulation methods of manual pouring and automatic stirring. The results from these experiments showed that the measured concentration of nano-sized fumed silica increased with the use of cyclone. This may attribute to the residual particles remained inside the cyclone or attached on its wall in the particle separation process, which needs to be considered in and the corresponding correction should be made when measuring the concentration of fumed silica with an instrument that uses a cyclone as a pre-separator.

KEYWORDS: *Fumed Silica, Deagglomeration, Cyclone, Real Time Instrument, Sampling*

INTRODUCTION

Materials, manufactured as a powder, often exist in two forms of a primary particle and agglomerate or aggregate of many particles. Primary particles are singular particles that are often less than one micron in diameter, while agglomerate or aggregate particles are a group of primary particles attached to each other [1-2]. These agglomerates are held together with weak intermolecular forces, such as Van der Waals, electrostatic, or mechanical forces. Among other causes, the presence of water or humidity can also be a driving force for agglomerate formation [1-2]. These forces are particularly effective at binding submicron particles with high surface area to volume ratios [1, 2]. Nanometer-sized fumed silica is a material with a primary size typically in the range of 7-14 nm [3-5]. It is used as an additive in the manufacturing of products, such as insulation panels, sealants, and golf balls. Workers, who use or produce fumed silica, can be exposed to it at the time of adding raw material in the manufacturing process of these items. In 1977, Vitums et al. [6] found that workers, who had long been exposed to fumed silica, suffered from histologically-documented pulmonary fibrosis and granulomatous nodules. Exposure to quartz, containing crystalline silica, is of most concern; however, investigators have also identified potential health effects associated with non-crystalline silica (amorphous) [3]. It has been found that human lung cells, exposed to fumed silica, caused an increase in reactive oxygen species (ROS) and lactate dehydrogenase (LDH) leakage from the cell membrane [3]. Researchers have also observed that exposure to those fumed silica p-articles in the micron and submicron size ranges can elicit the interleukin 1ß (IL-1ß) response [7-9]. This response is important because inflammasome activation has long been considered as an important mechanistic pathway for silica-induced lung diseases, such as silicosis. These diseases are

Corresponding author: Candace S.J. Tsai
Email: *Candace.Tsai@colostate.edu*

almost exclusively associated with crystalline silica, but it was found that some types of amorphous silica, fumed silica, could also induce inflammasome activity. The findings of these studies are further corroborated by the work of several other researchers [10, 11].

Direct-reading real-time instruments are important tools for gauging airborne concentrations of particles and nanomaterials that are recently and commonly used in both industrial and research fields. Some instruments are equipped with the components for pre-separation of particles as a way to ensure that only the particles in the measurable size range enter the instruments. A cyclone separator, as discussed in this study, removes and separates particles from a gas stream for size classification by drag, centrifugal, and buoyant forces, without using filtration methods [12]. Because of the simple structure and low maintenance and operating expenses, cyclones are commonly used in industries [13]. The physical characteristics of cyclones have been studied extensively. Yuu et al. found that as moving particles attach themselves to the cyclone walls; they increase the friction factor of the walls and decrease the tangential velocity. Yuu et al. concluded that the dust layer on the cyclone walls could cause a pressure drop [14]. Other researchers have studied the collection efficiency, possible pressure drop, and flow pattern, as well as the impact of these factors on the cyclone performance [13-16-18]. The influence of dust loading on the cyclone performance has also been studied [18]. The cyclone pressure drop for the solids-laden air flow was found to be about 47% of that for the clean air [17]. Hiraiwa et al. found that the 50% cut size with the free air inflow cyclone is smaller than that without the free air inflow cyclone, under the same pressure drop condition [15]. The effects of apex cone shape on the particle separation performance of gas-cyclones have been studied [16, 19]. It has been found that particle collection efficiency increased with an increase in the secondary flow rate and the number of secondary flow injection in the upper cylindrical part of the cyclone [16]. The effects of apex cone shape on the performance of the particle separation decreases under high inlet velocity conditions, because most particles are moving in the area away from the apex cone [19]. Although many studies have been done on the cyclone performance, due to the complexity of the particle separation mechanism, questions about how cyclones affect instrument measurements remain unanswered. Additionally, some differences have been observed between the measurements performed by the nano-scan Scanning Mobility Particle Sizer (SMPS) (TSI 3910), equipped with a cyclonic separator, and the SMPS (TSI 3936), which does not have the separator [20]. Researchers found that the results of nanoscan SMPS measurements showed higher concentrations. They also observed a larger number of small particles included in the nanoscan SMPS distribution [20]. It was hypothesized that this may be due to the presence of the cyclonic separator, acting as a disperser of weakly agglomerated particles, which results in the increased concentration of the particle and decreased mean particle size. Kousaka et al. found that particle agglomerate dispersion could be caused by acceleration or deceleration of an airstream and obstacles in the airstream [21].

The accuracy of measurement instruments is important for characterizing the true occupational and environmental exposure to contaminants and particle emissions. The primary focus of the relevant previous publications has been on the physical characteristics of cyclones and only a few studies have investigated the effect of cyclones on the measured particle concentrations and size distributions. The purpose of this study was to further characterize these effects in direct-reading real-time instruments.

MATERIALS AND METHODS

Experimental Media and Instruments: This study used the insulation raw material of fumed silica, which is commonly used in many industries for its low thermal conductivity and thixotropic properties. The fumed silica (CAS-No.112945-52-5) contained 90 to 100% concentration pyrogenic colloidal silica and was manufactured by pyrolysis (Sigma-Aldrich, St. Louis, MO). For each experiment, eight grams of silica was used.

Three instruments were compared in terms of measuring the airborne fumed silica particles; the nanoscan SMPS (Model 3910, TSI, Shoreview, MN, USA), Optical Particle Sizer (OPS) (Model 3330, TSI), and Fast Mobility Particle Sizer (FMPS) (Model 3091, TSI). The nanoscan SMPS, which measures the particles in the size range of 10 to 420 nm in 13 size channels, operates at 0.9 L/min. The OPS, which measures particles in the size range of 0.3 to 10 um in 16 size channels, operates at 1.0 L/min. The FMPS, which measures particles from 5.6 to 560 nm in 32 size channels, operates at 10 L/min. The maximum concentrations that can accurately be measured by the OPS, nanoscan SMPS, and FMPS are 3,000 particles/cm3, 1,000,000 particles/cm3, and 10,000,000 particles/cm3, respectively. The operating principle varies depending on the instruments. The OPS counts particles by measuring the intensity of light refraction created by the particles inside the optical chamber. The nanoscan SMPS counts particles by charging them as they enter the instrument and then, using isopropyl alcohol, condenses the particles to the size measurable by a spectrometer. The FMPS

Published online: August 30, 2018

counts particles by applying a charge to particles as they enter the instrument. The electrode in the device has a positive charge, which repels the particles toward the electrometer. Then, the particles are measured based on the place they hit on the electrometer. In this study, the nanoscan SMPS and FMPS were evaluated with and without cyclone to determine the effect of the cyclone on particle measurements. The OPS does not use a cyclone and serve as a control.

Sampling Enclosure and Particle Collection: All the experiments were run inside a glovebox that is equipped with an ultra-filter (manufactured by Terra Universal, Fullerton CA, USA). The dimensions of the glovebox were 89 cm. x 61 cm x 64 cm. The airflow, measured at the sampling location, was 0.01-0.07 m/s in the horizontal direction and 0-0.03 m/s in the vertical direction. A sampler, designed for collecting nanoparticle and respirable particles, called Tsai diffusion sampler, was used to collect the particles and confirm the presence of airborne fumed silica [22]. The particles were collected on a silica dioxide filmed, copper transmission electron microscope (TEM) grid, and a 25-mm polycarbonate filter with 0.2 μm pores, by Brownian motion/diffusion and sieving (for micron particles). The particle samples were collected at 0.3 L/min using a Gilian GilAir-3 personal air-sampling pump.

Experimental Process: Two generation methods of manual pouring and automatic stirring were used to determine the effectiveness of the instruments. Each method was conducted three times with and for three times, without the cyclone. The experiments lasted forty minutes. The first method, manual pouring, was done by pouring eight grams of fumed silica between two 240-mL natural polypropylene jars. The frequency of pouring was roughly four times per minute that lasted for ten minutes in total. The powder was poured at the brim of the jar for roughly five seconds each time.

For the second method, automatic stirring, eight grams of fumed silica was poured inside a 240 mL natural polypropylene jar and stirred for ten minutes with an automatic agitator (Model 50006-03, Cole-Palmer) at 400 rpm. During particle generation, the particle sampler and direct-reading instruments simultaneously collected the particles and recorded the data. The experimental setups for stirring and pouring are shown in Fig. 1a and b, respectively. The six distinct measurement points are shown in Fig. 2. At the end of each experiment, the glovebox was thoroughly decontaminated and all the samplers were removed. The instrument data was then collected for ten minutes, while no aerosol generation was occurred inside the glovebox. The OPS, nanoscan SMPS, and diffusion sampler were placed 5 cm away from the rim of the jar, and the FMPS was placed 10 cm away from the jar. The FMPS was placed farther from the place of particle generation because of its significantly higher flow rate (10 L/min) compared to the other devices used in the experiment (<1 L/min). The grids from the particle sampler were analyzed through TEM analysis. The OPS was used for a side-by-side comparison of the measurement variation as this instrument does not use a cyclone.

Evaluation of Real-Time Instrument Measurements: The data recorded by the instrument was exported from the device-specific application to the Microsoft Excel and then, analyzed. To demonstrate the differences between the measurement results of the instruments, four types of graphs were generated from the instrument data. 1) The particle count versus diameter figures were generated using the average particle count for each instrument size channel during the pouring or stirring activities. 2) The particle count percentage versus diameter distribution was generated by calculating the percentage of the particles measured by each size channel in the instrument. The distribution graphs was prepared to examine the size distribution differences between the experiments. 3) A total concentration versus time graph was also generated for each experiment and instrument to provide additional information about the particle concentrations throughout each experiment. 4) The plot of the cumulative percentage of particle count versus diameter was used to interpret the aerosol size distribution. Most of the presented figures displayed the data of the experimental period during the fumed silica manipulation (stirring/ pouring) and the post-experiment measurements.

Evaluation of Particle Images Taken by Electron Microscopy: the particles collected on the grids were analyzed using TEM to determine the existence and morphology of the particles from each sample. This analysis was performed by a JEOL JEM2100F TEM at 200 kV. Twenty images of grid spaces, containing low, medium, and high particle densities, were taken from each TEM grid to ensure that the images that could be a representative of the particle distribution were taken from each sample.

Once the images were taken, they were analyzed using FIJI image analysis software [23]. Analysis by this software provided information on the size and number of particles and allowed the researchers to evaluate the distribution of all the collected particles. To determine the particle size distribution using FIJI software, a contrast threshold was applied to each image; which eliminated background and allowed to count the particles individually.

Published online: August 30, 2018

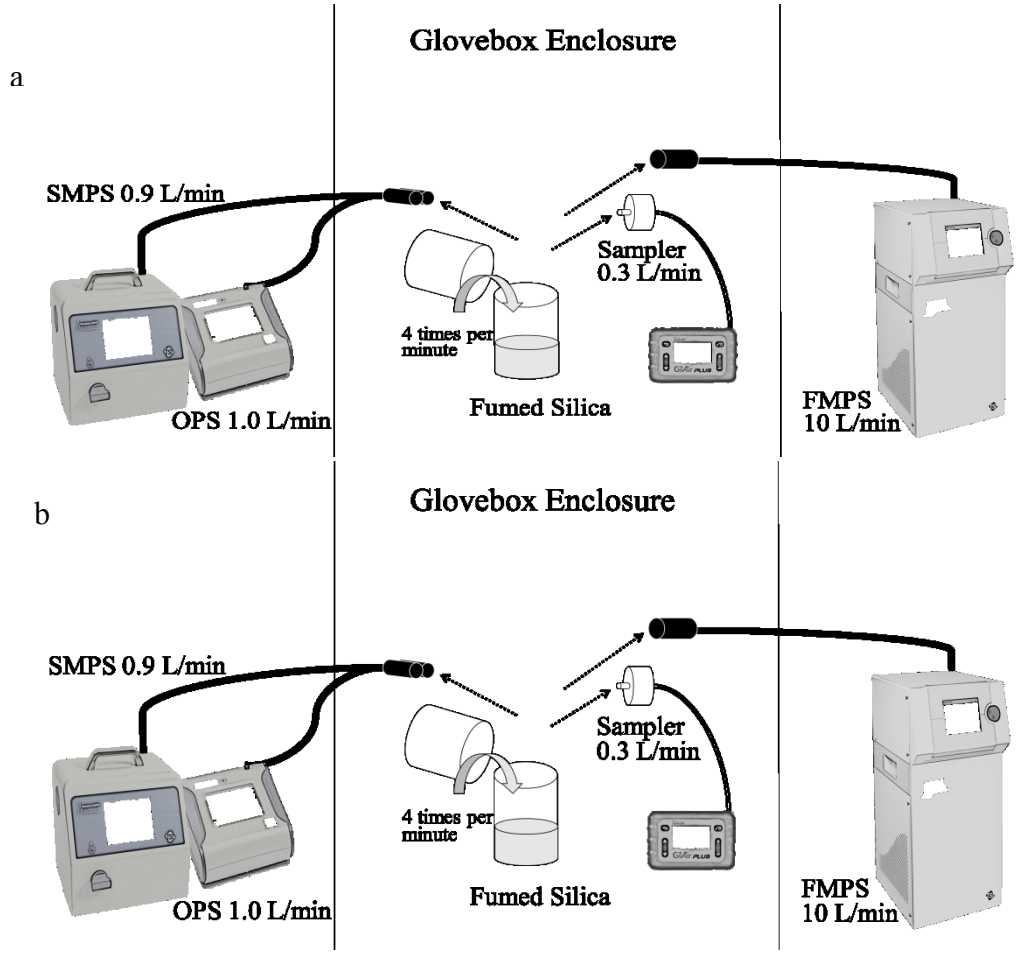

Fig. 1. Experimental designs for both particle generation methods. a) Experimental design for the stirring process, b) Experimental design for the pouring process.

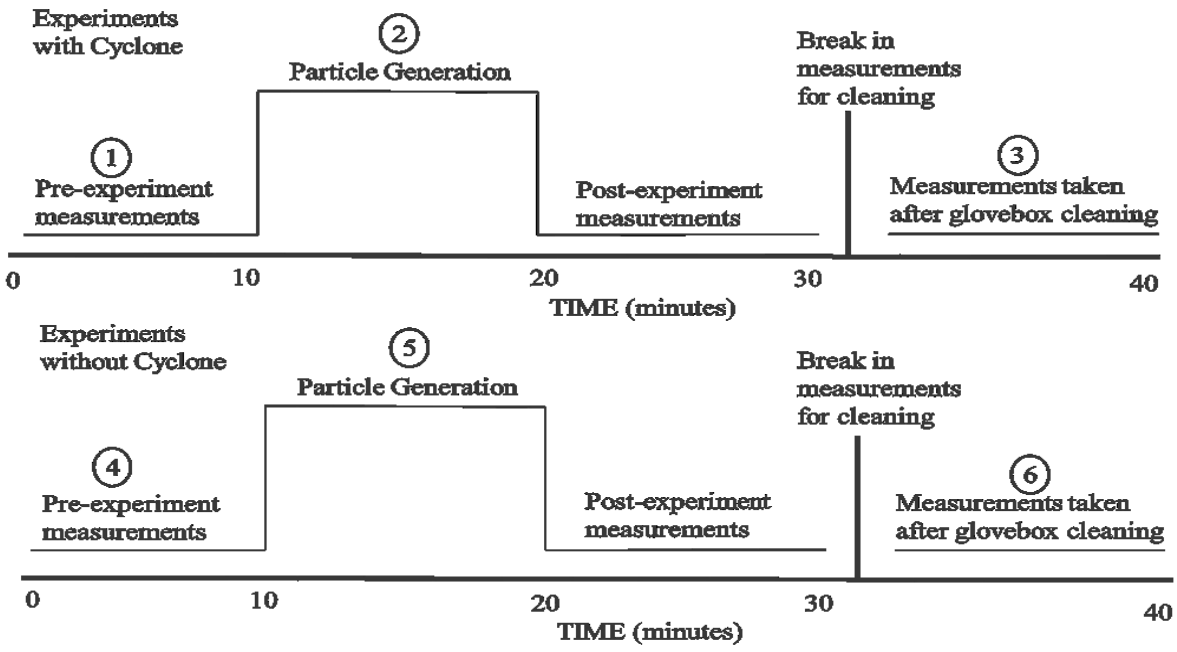

Fig. 2. Experimental procedure diagram
Note: Numbers 1 to 6 represent the measurement periods.

Published online: August 30, 2018

Once the threshold was applied, FIJI calculated the area of each particle, which was then converted to the equivalent circular area diameter. The analyzed particles were sorted into 27 size bins and counted. The particles, collected on the polycarbonate filters, were analyzed using a JEOL JSM-6500F Scanning Electron Microscope (SEM) at 15 kV. A total number of 20 images were taken from each sample, and the images were analyzed by FIJI using the same process, described for TEM images.

Statistical Analysis: The paired t-test was used to compare the particle diameters at the 50% cumulative concentration (D_{50}) and the particle modes between the runs with and without the use of cyclone as well as the two particle generation methods. The D_{50} represents the median particle diameter measured during each run. In this paper, the D_{50} was referred to as the relative D_{50} for each instrument measuring the particles in its size channel. It shows the size channel closest to the cumulative 50% of all the particles measured.

Paired t-tests were also used to compare the concentration differences between the runs with and without the use of cyclone. In better words, the tests were used to determine any significant differences in the total concentrations measured between the runs with and without the cyclonic separator. The differences in the measured concentrations before particle generation and after cleaning the glovebox (respectively in the pre- and post-experiment stages) were also tested. The P-values, obtained from the paired t-tests, were compared at an alpha level of 0.05. All of the statistical analyses were conducted in RStudio, an extension of R.

RESULTS AND DISCUSSION

Cyclone Effect during Experimental Process: The particle concentrations and size distributions measured by the instruments with and without the cyclone separator were compared. The data presented in Figs. 3 and 4 show the average particle counts in each bin range measured by the nanoscan SMPS and FMPS in both experimental processes with and without the cyclone separator. The data in these figures show the average size distribution during the particle generation, marked as numbers 2 and 5 in Fig 2. There were observed no clear trends in the particle distribution. However, there was found disparities in the total concentrations under the conditions of the use and non-use of cyclone separator, and between the experimental processes.

During the experiments, the majority of the particles recorded by the nanoscan SMPS were between 30 nm and 360 nm in diameter (Figs. 3a and 4a) and ranged between 50 nm and 400 nm for the particles measured by the FMPS (Fig. 3b and 4b). These ranges were relatively consistent in all runs. However, the mode sizes of the particles taken by the nanoscan SMPS and FMPS changed between the experiments with and without the cyclone separator. The modes for the nanoscan SMPS measurements in the conditions of the use and non-use of the separator were 170 nm and 160 nm, respectively (Figs. 3a and 4a). The modes for the FMPS measurements in the use and non-use of the cyclone separator ranged between 140 nm and 160 nm, respectively (Figs. 3b and 4b). The p-values were respectively 0.80 and 0.34 for the nanoscan SMPS and FMPS, which were not statistically significant. Supplementary Information (SI) (Figs. S1-S4) provides additional information on the cumulative distributions and diameter of the particles in the conditions with and without the use of cyclone separator as well as the cumulative distribution functions for each post-experiment analysis. The D_{50} of the measured particles can also be found in these figures.

Effect of Particle Generation Method: In this paper, the effect of particle generation methods on particle distribution was investigated. There were found differences in the distribution of the particles between the stirring and pouring methods. However, none of the observed differences were significant statistically. The D_{50} values of the particles measured by the nanoscan SMPS during the stirring and pouring activities under the condition of the use of cyclone separator were 116 nm and 154 nm (Fig. S1), respectively (p-value: 0.67). In the non-use of cyclone separator, the relative D_{50} was exactly opposite, 154 nm during the stirring activities and 116 nm during the pouring activities (Fig. S1) (p-value= 0.29). The D_{50} values of the particles measured by the FMPS during the stirring and pouring activities under the condition of the use of cyclone separator were 124 nm and 143 nm (Fig. S2), respectively (p-value= 0.42). When the cyclone was not used, the relative D_{50} was 143 nm (Fig. S2) for both stirring and pouring activities (p-value=0.42). None of the observed differences in the D_{50} values were statistically significant, indicating that the particle generation methods did not affect the particle size of the generated aerosol.

Post-cleaning Concentration and Distribution Results: After running the experiments and cleaning the glovebox, it was found that the size of the majority of the particles recorded by the nanoscan SMPS and FMPS ranged between 20-275 nm and 50-300 nm (Figs. S3 and S4), respectively. The average mode particle size, measured by the nanoscan SMPS after cleaning the glovebox, did not vary significantly between the experiments with the use and non-use of the cyclone

Published online: August 30, 2018

separator. The average of the modes was about 55 nm (p-value: 0.74) (Fig. S3). The average-mode particle size, measured by the FMPS, varied significantly between the experiments in the use and non-use of the cyclone separator. The mode particle size, measured by the FMPS after cleaning the glovebox, was 52 nm and 8.0 nm, respectively under the condition of the use and non-use of the cyclone separator (Fig. S4), (p-value=0.004). In addition to mode particle size, the D_{50} is also useful for determining the distribution of the measured particles. After cleaning the glovebox, the relative D_{50} values, measured by the nanoscan SMPS during the stirring experiments with and without the use of the cyclone, were 49 nm and 65 nm (Fig. S3a), respectively. There was found no statistically significant difference between these values (p-value=0.80). For pouring experiments, these values were 37 nm (Fig. S3b) for both runs with and without the cyclone separator (p-value=0.75). For the FMPS, after the glovebox was cleaned, the relative D_{50} measured during stirring experiments with and without the cyclone, were 52 nm and 34 nm (Fig. S4a), respectively (p-value=0.65). These values, for pouring experiments, were 93 nm and 22 nm (Fig. S4b) with and without the use of cyclone (p-value=0.01).

This measurement, in addition to the difference in the mode particle size measured by the FMPS, were the only statistically significant findings pertaining to the particle size distribution differences after the glovebox was cleaned. The significant decrease in median and mode particle size measured by the FMPS when the cyclone was not used was unexpected as it deviates from the hypothesis that the cyclone would break agglomerated particles into smaller particles.

As summarized in Table 1, the FMPS and nanoscan SMPS recorded greater concentrations after cleaning the glovebox in the conditions of the use of cyclone separator compared to the condition of post-experiment and non-use of cyclone separator. When the cyclone was used, during the no aerosol generation period, the average nanoscan SMPS concentration, recorded in the glovebox after the stirring and pouring experiments, was 1.3 x 10^3 particles/cm^3 and 1.2 x 10^3 particles/cm^3, respectively.

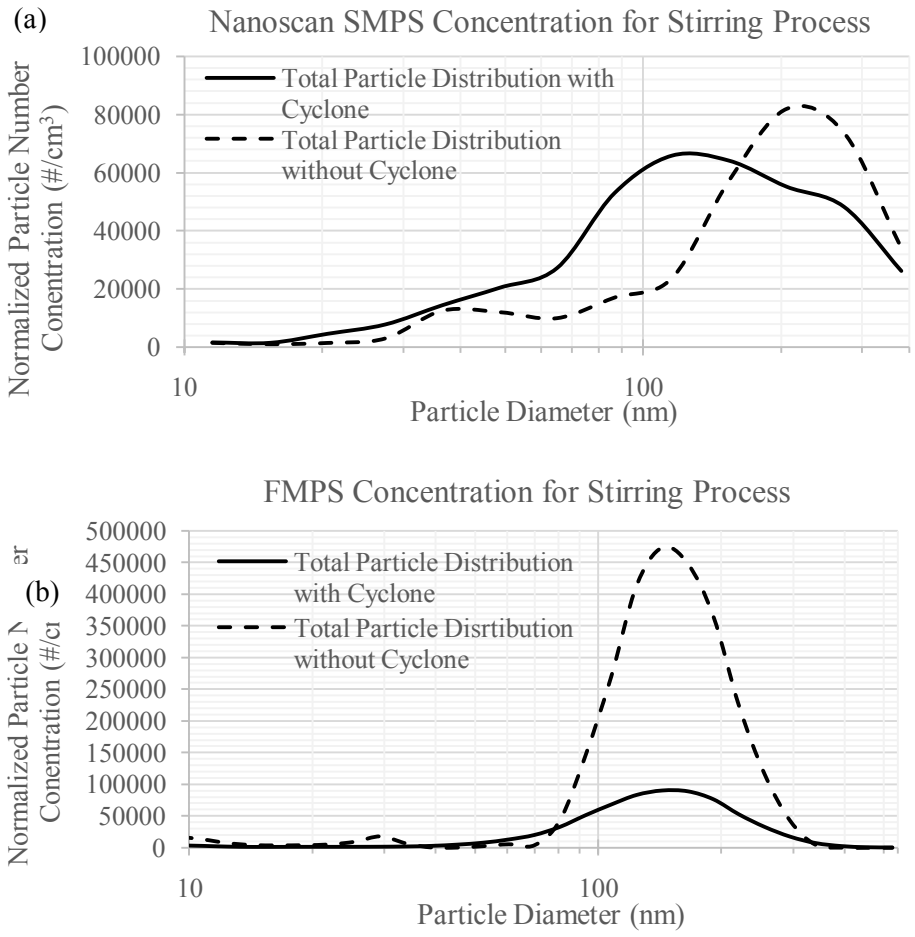

Fig. 3. Average particle concentration measured by a) nanoscan SMPS and b) FMPS during all of the stirring process runs. Note: Size range is 5 nm-560 nm for the measurements by FMPS, and 10 nm-420 nm for the measurements by nanoscan SMPS.

Published online: August 30, 2018

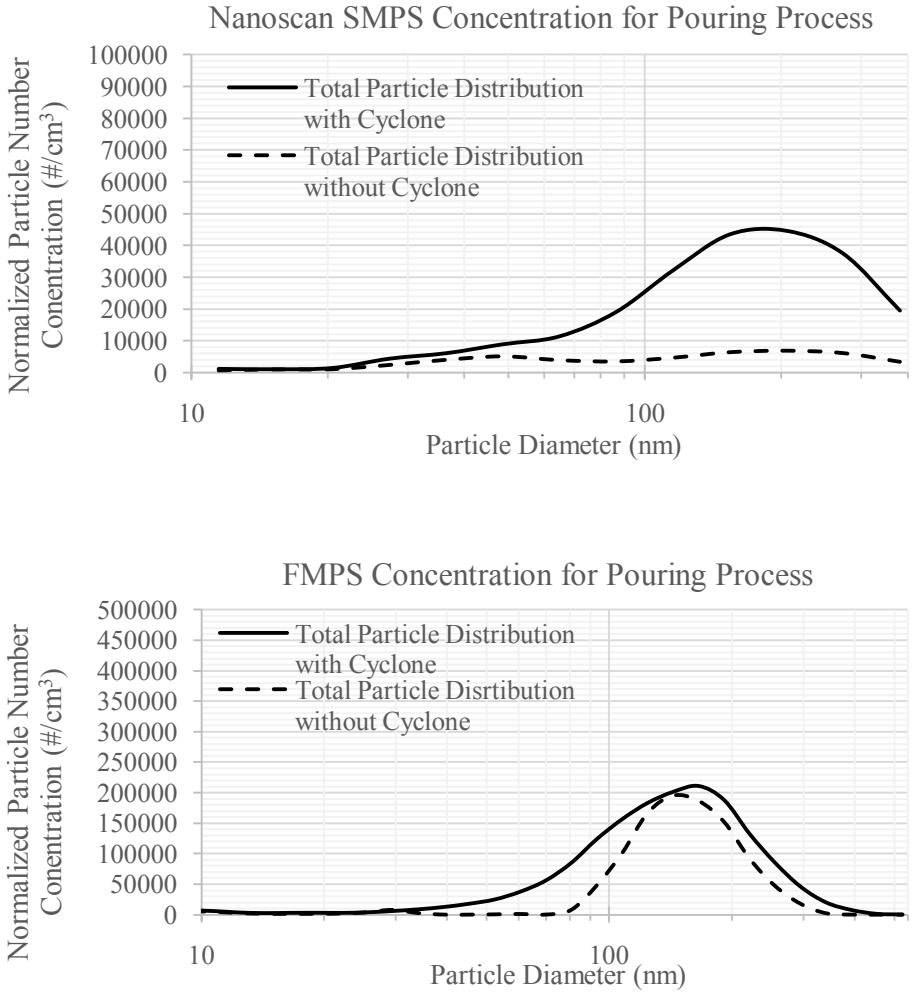

Fig. 4. Average particle concentration measured by a) nanoscan SMPS and b) FMPS during all pouring process runs.

Table 1. Average total particle number concentration for all runs

Experimental Process	**Presence of Cyclone (On SMPS and FMPS)**	**Total Concentration (#/cm^3)**		
		OPS	Nanoscan SMPS	FMPS
Stirring	Cyclone	210(±46)	5,000(±7,400)	43,000(±8,300)
	No Cyclone	750(±400)	40,000(±18,000)	170,000(±100,000)
Pouring	Cyclone	360(±290)	28,000(±32,000)	100,000(±110,000)
	No Cyclone	620(±280)	4,900(±1,500)	67,000(±34,000)
Post-Expt. Stirring	Cyclone	1.1(±1.6)	1,300 (±2,000)	11,000(±10,000)
	No Cyclone	0.9(±0.4)	51(±61)	500(±290)
Post-Expt. Pouring	Cyclone	0.6(±0.7)	1,200(±1,800)	25,000(±21,000)
	No Cyclone	0.2(±0.1)	110(±75)	860(±390)

Published online: August 30, 2018

When the cyclone was not used, the nanoscan SMPS recorded 51 particles/cm^3 and 110 particles/cm^3 during the no aerosol generation period and after the stirring and pouring experiments, respectively. Likewise, in the condition of the use of cyclone, the FMPS recorded 1.1 x 10^4 particles/cm^3 and 2.5 x 10^4 particles/cm^3 during the no aerosol generation period and after the stirring and pouring experiment. Under the condition of the non-use of the cyclone, the FMPS recorded 500 particles/cm^3 and 860 particles/cm^3 during the no aerosol generation period after stirring and pouring experiments, respectively. This indicated that the contamination from the cyclone separator had an effect on the particle concentrations measured by the nanoscan SMPS and FMPS as the residual particles are likely to be deagglomerated in the cyclone. Standard deviations of the average concentrations measured in all of the three runs are included in Table 1 per experiment type. It should be noted that the standard deviations are relatively large, which can be attributed to the fluctuating nature of the practical particle generation process. When the cyclone was not used, the nanoscan SMPS recorded 51 particles/cm^3 and 110 particles/cm^3 during the no aerosol generation period and after the stirring and pouring experiments, respectively. Likewise, in the condition of the use of cyclone, the FMPS recorded 1.1 x 10^4 particles/cm^3 and 2.5 x 10^4 particles/cm^3 during the no aerosol generation period after the stirring and pouring experiment. Under the condition of non-use of the cyclone, the FMPS recorded 500 particles/cm^3 and 860 particles/cm^3 during the no aerosol generation period after stirring and pouring experiments, respectively. This indicated that the contamination from the cyclone separator had an effect on the particle concentrations measured by the nanoscan SMPS and FMPS because the residual particles are likely to be deagglomerated in the cyclone. Standard deviations of the average concentrations measured in all of the three runs are included in Table 1 per experiment type. It should be noted that the standard deviations are relatively large, which can be attributed to the fluctuating nature of the practical particle generation process. These processes involved high variability, as they require periodic human intervention to continuously generate particles. Average particle concentrations over time are also presented in the SI (Fig. S5). These figures show how the concentration was variable throughout each experiment.

To test the accuracy of this finding, an additional t-test was done on each data set to test any significant difference between the runs with and without the use of the cyclone. The data are summarized in SI, Table 1. Based on the significant value of 0.05, there was found a statistical difference between the data sets of all runs with and without the use of cyclone. Additionally, almost all of the runs with the cyclone had higher particle counts compared to the runs without the cyclone. This corroborates the hypothesis that cyclone breaks large particle agglomerates into the smaller particles and therefore, causes a detectable increase in the measured concentration of particles. However, during the second run of the stirring experiments when the cyclone was not used, the FMPS measured higher particle concentrations than the non-use of cyclone. The same was also observed during the second run of the pouring experiments when the nanoscan SMPS recorded higher particle concentrations in the presence of cyclone compared to the non-use of the cyclone. These results indicate that the process is highly dependent on how the operator handles the sample during the particle generation. This shows how materials would be handled in the work environment.

There was also found a statistically significant difference between all of the OPS runs, except for the second set of the stirring experiments ($p < 0.05$). This was expected due to the consistent differences in the particle counts at low concentrations (Table 1). The effect of the use of cyclone separator is shown in the mean particle count difference of each instrument. The nanoscan SMPS and FMPS usually had higher particle counts in the presence of the cyclone separator (except for one cause in the FMPS stirring comparison). The difference in the particle counts ranged from 60 to 3.5 x 10^3 particles/cm^3 for the nanoscan SMPS to 90 to 4.8 x 10^4 particles/cm^3 for FMPS. The OPS recorded higher particle counts for three out of the six comparisons where the FMPS and nanoscan SMPS did not have the attached cyclone. The mean difference was minimal in the particle counts ranged from 0.5 to 3.4 particles/cm^3. Although every run was statistically different from its paired equivalent, the large discrepancy in the mean particle counts between the OPS and the other instruments provided further evidence on the contribution of cyclone in particle counts. The maximum particle count difference recorded by the OPS (3.4 particles/cm^3) could be due to the small differences in the thorough cleaning of the glovebox. However, the differences in many of the particle counts recorded by the other instruments were so large. It is very unlikely that the cleaned glovebox has so many residual particles to create such a large difference.

Comparison of Pre-experiment and Post-cleaning Measurements: In this section, a comparison is provided on the concentration measurements taken before the particle generation and after cleaning of the glovebox. This is a comparison between the points 1 and 3, and the points 4 and 6 in Fig. 2. The data presented in this section show differences in

the measured concentrations in the clean glovebox before and after each experiment. This allows for a comparison of the instrument measurements taken by a clean cyclone and a contaminated cyclone in the clean glovebox. In the runs with the presence of cyclone separator, the cyclone was cleaned prior to the particle generation, but not before decontaminating of the glovebox. The results of the measurements in the use and non-use of the cyclone separator were also compared. During the stirring runs, when the cyclone was used, the nanoscan SMPS and FMPS measured an average of 1,150 and 10,600 particles/cm^3, respectively. The counted particles in the post-experiment step after cleaning the glovebox, when the cyclone was contaminated, was higher than that before the particle generation, when the cyclone was clean. During the pouring runs, when the cyclone was used, the nanoscan SMPS and FMPS measured an average value of 1,060 and 24,900 particles/cm^3 respectively. The counted particles after cleaning the glovebox were higher than that before particle generation. During the stirring experiments, when the cyclone was not used, the nanoscan SMPS and FMPS measured an average of 88 and 12 particles/cm^3, respectively. The counted particles after cleaning the glovebox were fewer than that before the particle generation. During the pouring experiments, when the cyclone was not used, the nanoscan SMPS and FMPS measured an average of 50 and 714 particles/cm^3, respectively. The counted particles after cleaning the glovebox were more than that before the particle generation. The number of particles measured before the particle generation and after the glovebox cleaning in the presence of cyclone separator was significantly larger than when the cyclone was not used. This comparison provided further evidence on the fact that the residual particles trapped in the cyclone, including those attached on the cyclone wall, have a contribution in the measured concentrations [14]. Greater average concentrations before the particle generation were observed only during the pouring experiments when the cyclone was not used.

TEM and SEM Size Distribution Analysis: The diffusion sampler collects particles on a polycarbonate filter and a TEM grid. The pore size of the used filter was approximately 200 nm. This allows larger particles to mostly be impacted onto the filter, while smaller particles are primarily deposited onto the TEM grid due to Brownian motion. The use of the TEM grid together with filter allowed for a wide range of particles to be collected and analyzed. The images of the particles collected on the TEM grids are shown in Fig. 5a and b.

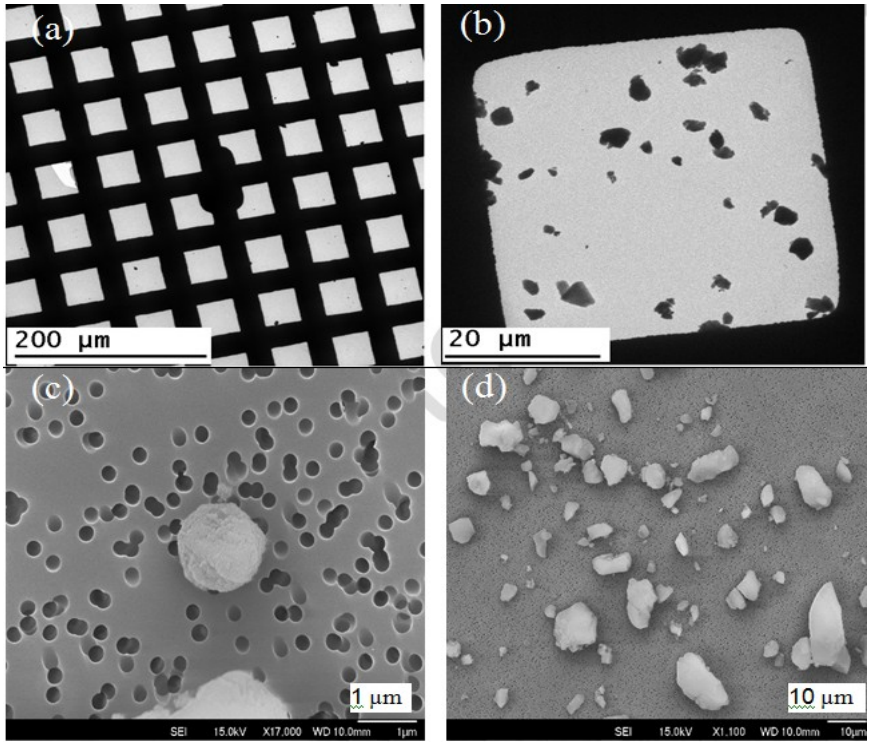

Fig. 5. Electron microscopy images. a) TEM image of the grid containing fumed silica particles on the silica dioxide film, b) TEM images of the fumed silica particles on the silica dioxide film of one grid space, c) SEM images of fumed silica on the polycarbonate filter, at a high-magnification view (x17,000), and d) SEM images of the fumed silica on the polycarbonate filter at a low-magnification view (x1,100)

Published online: August 30, 2018

These images show the fumed silica particles at various sizes. The majority of the particles collected by the particle sampler were in the size range of 12 nm to 337 nm. The D_{50} and mean particle diameter collected on the TEM grid was 115.5 nm. This range is comparable to that of the particles collected by the nanoscan SMPS and FMPS, which ranges from 20 nm to 300 nm. In addition, the median particle diameter measured by the nanoscan SMPS during the stirring with the cyclone and pouring without the cyclone was identical to that collected on the TEM grid.

The SEM images taken from the particles collected by the diffusion sampler onto the filters are shown in Fig. 5c and d. It was found that the collected filter particles by the diffusion sampler were in the range of 11.5 nm to 16 μm; majority of which ranged between 400 nm and 9 μm. The values of mean particle diameter collected on the filters and D_{50} were 2,800 nm and 1,300 nm, respectively. The data from the instruments did not include many of the particles whose size was greater than 400 nm. The presence of these particles on the particle sampler filter indicated that the instruments potentially underestimate the number of large particles, which may be due to the deagglomeration in the cyclone.

This data further verifies the measurements taken by the instruments as the D_{50} and size range of fumed silica particles collected on the TEM grids were similar to that by the nanoscan SMPS and FMPS. However, the SEM images of the filters showed that the concentration of the particles greater than 400 nm was likely to be underestimated by the instrument measurements.

CONCLUSION

After cleaning the glovebox, there were found statistically significant differences in the measured concentrations between the experimental runs in the presence and absence of the cyclone separator. The higher post-experiment concentrations in the presence of the cyclone separator were attributed to the residual particles trapped in the cyclone. The cyclone, by removing larger particles from the sampling, greatly affected the measurements of fumed silica taken by the studied instruments. The results of this study help filling the knowledge gap regarding the accuracy of the measurements taken by direct-reading instruments and the association of this to the monitoring of occupational exposure. It is recommended to correct the measured values when measuring the particles that can be deagglomerated. This can be done by subtracting the residual concentration from the total concentration measured. It is also suggested that a small high-efficiency particulate air (HEPA) filter unit, which is usually available for instrument calibration, be connected to the air inlet of the instruments equipped with a cyclone separator to gauge the concentration of the residual particle inside the cyclone after finishing the experiment. This value can be subtracted from the measured values to obtain real concentrations.

ACKNOWLEDGMENTS

The authors would like to thank Daniel Theisen for his assistance in the experiments and microscopic analysis. This research study was sponsored by Aspen Aerogels, Inc. and the Centers for Disease Control and Prevention (grant number: 5T42OH009229-11). The authors have no completing interests.

REFERENCES

1. Hartley PA, Parfitt GD, Pollack LB. The role of the van der Waals force in the agglomeration of powders containing submicron particles. *Powder Technol* 1985; 42(1): 35-46.
2. Corn M. The Adhesion of Solid Particles to Solid Surfaces, I. a Review. *J Air Pollut Control Assoc* 1961; 11(11): 523-528.
3. Irfan A, Cauchi M, Edmands W, Gooderham N, Njuguna J, Zhu H. Assessment of Temporal Dose-Toxicity Relationship of Fumed Silica Nanoparticle in Human Lung A549 Cells by Conventional Cytotoxicity and H-NMR-Based Extracellular Metabonomic Assays. *Toxicol Sci* 2014; 138(2): 354-64.
4. Merkel TC, Freeman BD, Spontak RJ, He Z, Pinnau I, Meakin P, Hill AJ. Ultrapermeable, Reverse-Selective Nanocomposite Membranes. *Science* 2002; 296(5567): 519-522.
5. Raghavan S, Khan S. Shear-Thickening Response of Fumed Silica Suspensions under Steady and Oscillatory Shear. *J Colloid Interf Sci* 1997; 185(1): 57-67.
6. Vitums VC, Edwards MJ, Niles NR, Borman JO, Lowry RD. Pulmonary Fibrosis from Amorphous Silica Dust, A Product of Silica Vapor. *Arch Environ Occup Health* 1977, 32(2): 62-68.
7. Sandberg W, Lag M, Holme J, Friede B, Maurizio G, Kruszewski M, Schwarze P, Skuland T, Refsnes M. Comparison of non-crystalline silica nanoparticles in IL-1β release from macrophages. *Part Fibre Toxicol* 2012: 9(1): 32.
8. Ren L, Zhang J, Zou Y, Zhang L, Wei J, Shi Z, Li Y, Guo C, Sun Z, Zhou X. Silica nanoparticles induce reversible damage of spermatogenic cells via RIPK1 signal pathways in C57 mice. *Int J Nanomedicine* 2016; 24(11): 2251-64.
9. Sun B, Wang X, Liao YP, Ji Z, Chang CH, Pokhrel S, Ku J, Liu X, Wang M, Dunphy DR, Li R, Meng H, Mädler L, Brinker CJ, Nel AE, Xia T. Repetitive Dosing of Fumed Silica Leads to Profibrogenic Effects through Unique

Structure−Activity Relationships and Biopersistence in the Lung. ACSnano 2016; 10(8): 8054-66.
10. Kaewamatawong T, Kawamura N, Okajima M, Sawada M, Morita T, Shimada A. Acute Pulmonary Toxicity Caused by Exposure to Colloidal Silica: Particle Size Dependent Pathological Changes in Mice. *Toxicol Pathol* 2005; 33(7): 743-9.
11. Zhang H, Dunphy DR, Jiang X, Meng H, Sun B, Tarn D, Xue M, Wang X, Lin S, Ji Z, Li R, Garcia FL, Yang J, Kirk ML, Xia T, Zink JI, Nel A, Brinker CJ. Processing pathway dependence of amorphous silica nanoparticle toxicity: colloidal versus pyrolytic. *J Am Chem Soc* 2012; 134(38): 15790-15804.
12. Hinds WC. *Aerosol technology: properties, behavior, and measurement of airborne particles.* 2nd ed., Wiley-Interscience, England.
13. Yoshida H, Kwan-Sik Y, Fukui K, Akiyama S, Taniguchi S. Effect of apex cone height on particle classification performance of a cyclone separator. *Adv Powder Technol* 2003; 14(3): 263-278.
14. Yuu S, Jotaki T, Tomita Y, Yoshida K: The reduction of pressure drop due to dust loading in a conventional cyclone. *Chem Eng Sci* 1978; 33(12):1573-1580.
15. Hiraiwa Y, Oshitari T, Fukui K, Yamamoto T, Yoshida H. Effect of free air inflow method on fine particle classification of gas-cyclone. *Sep Purif Technol* 2013; 118:670-679.
16. Yoshida H. Effect of apex cone shape and local fluid flow control method on fine particle classification of gas-cyclone. *Chem Eng Sci* 2013; 85:55-61.
17. Fassani FL, Goldstein L. A study of the effect of high inlet solids loading on a cyclone separator pressure drop and collection efficiency. *Powder Technol* 2000; 107(1): 60-65.
18. Hoffmannc AC, van Santen A, Allen RWK, Clift R. Effects of geometry and solid loading on the performance of gas cyclones. *Powder Technol* 1992; 70(1): 83-91.
19. Yoshida H, Nishimura Y, Fukui K, Yamamoto T. Effect of apex cone shape on fine particle classification of gas-cyclone. *Powder Technol* 2010; 204(1): 54-62.
20. Yamada M, Takaya M, Ogura I. Performance evaluation of newly developed portable aerosol sizers used for nanomaterial aerosol measurements. *Ind Health* 2015; 53(6): 511-6.
21. Kousaka Y, Okuamama K, Shimizu A, Yoshida T. Dispersion Mechanism of Aggregate Particles in Air. *J Chem Eng Jpn* 1979; 12(2): 152-159.
22. Tsai C, Theisen D. A Sampler Designed for Nanoparticles and Respirable Particles with Direct Analysis Feature. *J Nanopart Res* 2018; 20(209).
23. Schindelin J, Arganda-Carreras I, Frise E, Kaynig V, Longair M, Pietzsch T, Preibisch S, Rueden C, Saalfeld S, Schmid B. Fiji: an open-source platform for biological-image analysis. *Nat Methods* 2012; 9(7): 676-682.

Published online: August 30, 2018